

# Safety enhancement in robotic neurosurgery through vessel tracking

S. Moccia<sup>1,2</sup>, F. Prudente<sup>2</sup>, E. De Momi<sup>1</sup>, C. Riviere<sup>3</sup>, A. Perin<sup>4</sup>, R. Sekula<sup>5</sup>,  
L. S. Mattos<sup>1</sup>

<sup>1</sup>*Department of Advanced Robotics, Istituto Italiano di Tecnologia, Genoa, Italy*

<sup>2</sup>*Department of Electronics, Information and Bioengineering, Politecnico di Milano, Milan, Italy*

<sup>3</sup>*Robotics Institute, Carnegie Mellon University, Pittsburgh, USA*

<sup>4</sup>*Besta NeuroSim Center, IRCCS Istituto Neurologico C. Besta, Milan, Italy*

<sup>5</sup>*Department of Neurological Surgery, University of Pittsburgh, Pittsburgh, USA*

[sara.moccia@iit.it](mailto:sara.moccia@iit.it)

## INTRODUCTION

Meningioma is a common type of primary intracranial neoplasm that arises from the middle layer of meninges. Surgery is the gold standard treatment for meningiomas, since it lowers patient mortality or after-treatment morbidity. Large vessel preservation and bleeding avoidance are of primary importance during the surgery, since they strongly influence surgical outcomes. Bleeding requiring transfusion is recognized as one of the most common complications (10.2%) [1].

The final goal of this research is to provide a tool for safety enhancement in robotic neurosurgery through vessel tracking.

During surgery, the primary imaging source to obtain a magnified view of both brain and cerebral vessels is microscopy (Fig. 1). Main challenges in vessel segmentation and tracking arise from partial or total vessel occlusion (e.g. due to surgical tools, smoke and saline solution).

A large literature on vessel segmentation and tracking algorithms exists, and a recent review can be found in [2], where algorithms are divided into (i) pattern recognition techniques, (ii) matched filtering, (iii) vessel tracking/tracing, (iv) mathematical morphology, (v) multiscale approaches, (vi) model-based approaches and (vii) hardware-based approaches.

In this paper, a Geometrical Deformable Model-based approach (GDM) is used to perform vessel segmentation in the microscopy frames, and Kalman filtering is used to track the segmentation between consecutive microscopy frames. The GDM initialization here proposed requires minimum manual intervention, which consists in the selection of two seed points in the first microscopy frame that are then automatically connected employing a Minimum Cost Path (MCP) algorithm.

## MATERIALS AND METHODS

The workflow of the proposed method is shown in Fig. 2. First, the user was required to initialize the segmentation algorithm by selecting two seed points,  $\mathbf{p}_1$  and  $\mathbf{p}_2$ , in the first microscopy frame. The seeds were then connected using a MCP algorithm [3]. MCP finds the curve  $C_{\mathbf{p}_1\mathbf{p}_2}$  that minimizes the cost path between  $\mathbf{p}_1$  and  $\mathbf{p}_2$ , according to a tensor metric  $M$ .

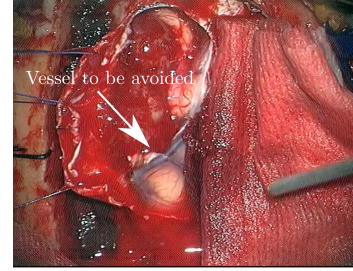


**Figure 1.** Microscopy frame recorded during meningioma surgery. The white arrow indicates the vessel to be avoided.

In order to drive the path evolution along the vessel main axis, an anisotropic  $M$  was built such that:

$$M = v * \Lambda * v^T$$

where  $v = [v_1; v_2]$ , with  $v_1$  and  $v_2$  image Hessian eigenvectors, and  $\Lambda = [\lambda_1 \ 0; 0 \ \lambda_2]$ , with  $\lambda_1 \leq \lambda_2$  image Hessian eigenvalues. The cost path minimization problem was solved through the computation of the Minimal Action Map (MAM), whose values can be interpreted as the arrival time of a propagation front that starts from  $\mathbf{p}_1$ , which is the only MAM minimum, and moves with velocity dependent on  $M$ . The minimum path was retrieved with gradient descent (Runge-Kutta) from  $\mathbf{p}_2$  on the MAM.

The  $C_{\mathbf{p}_1\mathbf{p}_2}$  was used to initialize a GDM. GDMs are well known to successfully face complex vessel architectures, such as bifurcation and vessel kissing, as well as image intensity drops and non-uniform illumination [2]. GDMs consider curves ( $\mathcal{S}$ ) that deform according to the curve-evolution theory described by:

$$\frac{\partial \mathcal{S}}{\partial t} = Z * \mathbf{n}$$

in which  $Z$  is called speed function and  $\mathbf{n}$  is the unit normal to  $\mathcal{S}$ . In this research, distance regularized level set [4] was used to implement the  $\mathcal{S}$  evolution since it guarantees the regularity of the level set ensuring stability during the evolution. The vesselness measure described in [5] was used to enhance vessels in each frame. The enhanced image was then used as speed function  $Z$ .

After having obtained the vessel segmentation

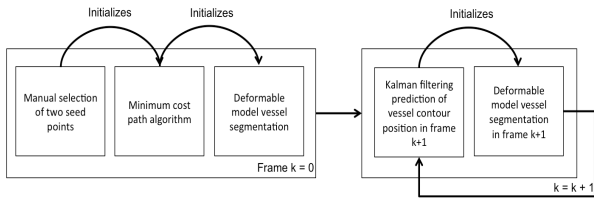


**Figure 2.** The workflow of the proposed algorithm for vessel segmentation and tracking.

in the first frame  $I_{k=0}$ , vessel tracking in the consecutive frames was performed exploiting Kalman filtering. For each frame  $I_{k,k>0}$ , the Kalman prediction of the vessel contour position provided the initialization for the  $\mathcal{S}$  evolution in that frame. The  $\mathcal{S}$  evolution was implemented using the GDM as in the first frame. The Kalman transition matrix was obtained by estimating the displacement between consecutive frames through Optical Flow (OF) [6].

Matlab<sup>®</sup> 2015b was used for the implementation of the described algorithms.

The proposed method was tested on a microscopy video recorded during a meningioma resection intervention at the Istituto Neurologico Carlo Besta, Milan, Italy. The patient gave informed consent.

## RESULTS

Vessel segmentation was numerically evaluated with respect to manual segmentation performed by an expert, elected as gold standard. The evaluation was done in terms of Accuracy (Acc), Sensitivity (Se) and Specificity (Sp), where Acc is the proportion of true results, both True Positive (TP) and True Negative (TN), among the total number of pixels. Se measures the proportion of positives, both TP and False Negative (FN), correctly identified. Sp measures the proportion of negatives, both TN and False Positive (FP), correctly identified. Segmentation results are: Acc = 0.99, Sp = 0.99 and Se = 0.67.

Fig. 3 shows (a) the MAM and (b) the resulting minimum cost path computed in the first video frame. Fig. 4 depicts (a) the speed function  $Z$  computed for the first frame and (b) the resulting segmentation obtained with the GDM. Fig. 5 shows (a) the OF computed for two consecutive frames and (b) the segmentation obtained for the second frame.

## CONCLUSION AND DISCUSSION

The proposed method showed to be able to face image noise, non-uniform illumination and intensity drops. The Kalman filtering successfully tracked the vessel contour, providing an automatic initialization for the segmentation in the consecutive frames. This way, the only user interaction required consisted in the selection of two seed points in the first frame.

This preliminary analysis on one video recorded during a real surgery showed the method to be effective.

Future work deals with real-time implementation. Moreover, the next step is the inclusion of OF-failure

recognition strategy to ensure accurate tracking in case of sudden and prominent field of view changes.

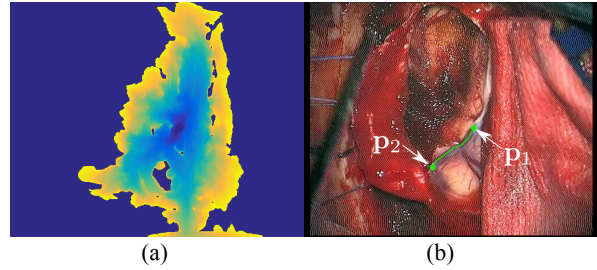


**Figure 3.** (a) Minimal action map computed for the first frame and (b) resulting minimum cost path. The white arrows indicate the two manually selected seed points.

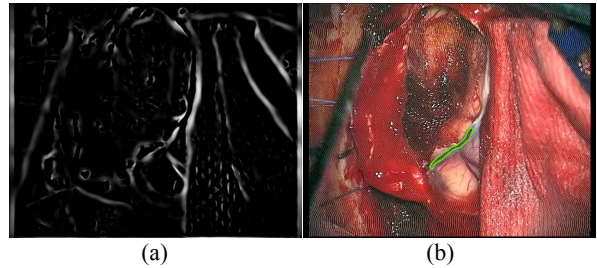


**Figure 4.** (a) Speed function for the geometric deformable model evolution. (b) Segmentation obtained for the first microscopy frame.

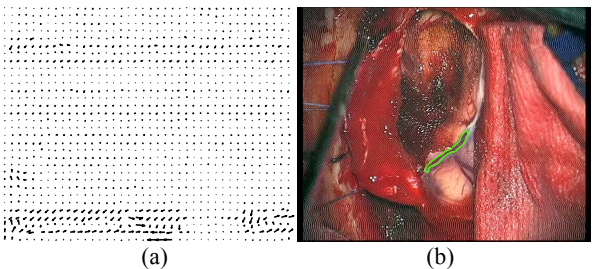


**Figure 5.** (a) Optical flow describing the displacement between the first and second frame. (b) Kalman prediction (white) and obtained segmentation (green) for the second frame.

## REFERENCES

- [1] Michalak S, et al., "Predictors of complications and mortality in cerebrovascular surgery," *Neurosurgery*; 2016.
- [2] Fraz MM, et al., "Blood vessel segmentation methodologies in retinal images—a survey," *Computer methods and programs in biomedicine*; 2015; 108(1): 407-433.
- [2] Deschamps T, et al., "Fast extraction of minimal paths in 3D images and applications to virtual endoscopy," *Medical image analysis*; 2001; 5(4): 281-299.
- [4] Chunming L, et al., "Distance regularized level set evolution and its application to image segmentation," *Image Processing, IEEE Trans on*, 2010; 19(12): 3243–3254.
- [5] Frangi AF, et al., "Multiscale vessel enhancement filtering," *Medical Image Computing and Computer-Assisted Intervention—MICCAI, 1998*; 130-137.
- [6] Sun D, et al., "Secrets of optical flow estimation and their principles," *Computer Vision and Pattern Recognition (CVPR), IEEE Conference on*, (2010), 2432-2439.